

# Substrate Roughness and Thickness Effects on Cold Spray Nanocrystalline Al-Mg Coatings

P. Richer, B. Jodoin, L. Ajdelsztajn, and E.J. Lavernia

(Submitted August 26, 2005; in revised form January 27, 2006)

Nanocrystalline Al-Mg coatings were produced using the cold gas dynamic-spraying technique. Unsieved Al-Mg powder of average nanocrystalline grain size in the range of 10 to 30 nm and with a particle size distribution from 10 to >100  $\mu\text{m}$  was used as the feedstock powder. The resulting coatings were evaluated using scanning electron microscopy (SEM), transmission electron microscopy, as well as microhardness and nanoindentation measurements. Coating observations suggest that the wide particle size distribution of the feedstock powder has a detrimental effect on the coating quality but that it can be successfully mitigated by optimizing the spraying parameters. Nanohardness values close to 3.6 GPa were observed in both the feedstock powder and coatings, suggesting the absence of cold-working hardening effects during the process. The effects of the substrate surface roughness and thickness on coating quality were investigated. The deposited mass measurements performed on the coatings showed that the effect of using different grit sizes for the substrate preparation is limited to small changes in the deposition efficiency of only the first few layers of deposited material. The SEM observation showed that the substrate surface roughness has no significant effect on the macrostructures and microstructures of the coating. The ability to use the cold gas dynamic spraying process to produce coatings on thin parts without noticeable substrate damage and with the same quality as coatings produced on thicker substrates was demonstrated in this work.

**Keywords** aluminum alloy coatings, cold spray, nanocrystalline feedstock, substrate thickness, surface roughness

## 1. Introduction

Cold gas dynamic spraying, also referred to as cold spray, is a relatively new high-rate material deposition process. Originating from the observation of tracer particle build up during supersonic wind tunnel tests, it was first developed in the mid-1980s at the Institute of Theoretical and Applied Mechanics in Russia (Ref 1) and has since evolved into a promising coating technology.

Cold spray uses a supersonic gas flow in which powder particles (typically tens of microns in size) are accelerated above a critical velocity. On impact, the solid particles having sufficient velocity to deform plastically and bond (Ref 1, 2) to the substrate to form a coating. A wide variety of materials have been successfully sprayed such as copper, aluminum alloys, nickel alloys, WC-Co, zinc, and titanium, among others (Ref 2-8). As opposed to other thermal spray processes, cold spray does not involve any significant heating of the powder particles as the process temperature never reaches the melting temperature of

the sprayed material. One of the prevailing theories suggests that cold spray coatings are produced solely as a result of intense local plastic deformation (Ref 9-12), although some researchers have theoretically shown that localized melting is possible (Ref 13). Accordingly, cold spray is referred to as a solid-state process, which has been shown to yield significant advantages such as the inhibition of microstructural and chemical changes resulting in the preservation of mechanical and chemical properties of the original feedstock (Ref 8).

Given the absence of significant heating and its resulting grain growth mechanism, cold spray can be used to produce nanocrystalline coatings by using nanocrystalline feedstock (Ref 8, 14-17). When compared with conventional materials, nanocrystalline materials typically exhibit a significant increase in mechanical properties due to the increased number of atoms located at grain boundaries, thus improving the ability of the material to impede dislocation motion (Ref 18). Although other thermal spray methods such as plasma or high-velocity oxyfuel spraying have been successful in producing fine grain structures (80–200 nm) (Ref 19, 20), their high operating temperatures inevitably cause grain growth and some degree of oxidation. Cold spray thus offers the possibility of producing nanocrystalline coatings with enhanced properties compared with those of other conventional thermal spray methods.

As cold spray is still in its development phase, the effect of numerous operating parameters has already been investigated in an attempt to improve and ultimately optimize the process (Ref 21-24). In most thermal spray applications, the feedstock powder size distribution needs to be carefully controlled to achieve satisfactory coating quality. Powder particles are therefore typically produced and/or sieved to within a desirable size range prior to spraying. Additional costs associated with material waste and manufacturing time could be eliminated if the sieving

The original version of this paper was published in the CD ROM *Thermal Spray Connects: Explore Its Surfacing Potential*, International Thermal Spray Conference, sponsored by DVS, ASM International, and IIW International Institute of Welding, Basel, Switzerland, May 2-4, 2005, DVS-Verlag GmbH, Düsseldorf, Germany.

**P. Richer** and **B. Jodoin**, Department of Mechanical of Engineering, University of Ottawa, ON, Canada; and **L. Ajdelsztajn** and **E. J. Lavernia**, Department of Chemical Engineering and Materials Science, University of California, Davis, CA 95616-5294. Contact e-mail: jodoin@genie.uottawa.ca.

**Table 1 Mechanical properties of Al-6061-T651 alloy**

Property	Value
Ultimate tensile strength	310 MPa
Tensile yield strength	276 MPa
Modulus of elasticity	68.9 GPa
Ultimate bearing strength	607 MPa
Bearing yield strength	386 MPa
Brinnell hardness	95
Vickers hardness	107

procedure could be avoided. As such, this study aims to optimize the cold spray spraying parameters to produce high-quality coatings from unsieved nanocrystalline Al-Mg feedstock. Recent interest in this nanocrystalline alloy (due to its enhanced properties such as mechanical strength and thermal stability) was central to its selection for this study (Ref 25). Furthermore, this study addresses two issues associated with substrate characteristics. First, the coating process often requires extensive substrate surface preparation resulting in longer manufacturing times, environmental impacts, and higher costs. Second, some applications require coatings on thin and hollow components that may be susceptible to damage during the coating process. This study examines the effects of the substrate average surface roughness and thickness on the overall quality of cold spray coatings produced using unsieved nanocrystalline Al-Mg powder.

## 2. Experimental Procedure


### 2.1 Feedstock Powder Preparation

The as-received powder was spray atomized Al-7.6at.%Mg. The powder was then mechanically milled for 8 h at a rate of 180 rpm in a modified Union Process (Akron, OH) 01-ST attrition mill. Stainless steel balls (6.4 mm in diameter) were used as the grinding media with a ball-to-powder weight ratio of 32:1. Milling was performed under a constant supply of liquid nitrogen. This milling process is often referred to as cryomilling and has been shown to be one of many successful processes used to produce materials with a nanocrystalline microstructure (Ref 26).

### 2.2 Substrate Preparation

Prior to spraying, the substrates (made from commercial Al 6061-T651 6 mm thick flat bars) were cut to the desired dimensions (10 × 2 cm) and subjected to different surface preparations. General mechanical properties of this aluminum alloy are presented in Table 1.

It has been shown that the cold spray process requires minimal surface preparation: manual grit blasting is typically sufficient. As such, two types of commercially available grits were used: a coarse silica (quartz) grit with an average particle size of 686 μm (20-mesh, 24-grit); and glass bead (BT-6) grit with an average particle size of 254 μm (50-mesh, 60-grit). The average substrate roughness Ra was evaluated using a portable surface roughness tester (model SurfTest SJ-201P; Mitutoyo, Aurora, IL). Roughness measurements were performed in both the longitudinal and transverse directions relative to the substrate. The reported values are the average of 12 measurements for each sample. Thinner substrates were also used to examine the effect of substrate thickness on the overall coating quality and to de-



termine whether thin substrates are likely to be damaged during the cold spray process. The substrates for these trials were cut to size (10 cm in length by 2 cm in width) from a commercial 1 mm thick sheet of Al 6061-T651 alloy and were then manually grit-blasted on both sides with the silica (quartz) grit. These substrates were then positioned in the substrate holder such that their central portion was unsupported (both ends in fixed support configuration).

### 2.3 Cold Spray Facility

The nanocrystalline Al-Mg powder was deposited on the aluminum substrates using the cold spray system developed at the University of Ottawa Cold Spray Laboratory. The facility consists of a spraying chamber connected to two separate high-pressure gas supplies. Helium was used for this study. The primary gas line (driving gas) is connected to a converging-diverging nozzle within the spraying chamber to generate the required supersonic flow. The secondary high-pressure gas supply is connected to a commercially available powder feeder (model 1264; Praxair, Danbury, CT) that feeds the powder particles into the main flow. The substrate holder is motorized to enable the lateral motion of the substrate relative to the nozzle. Figure 1 shows a schematic of the cold spray facility used in this study.

The cold spray system is equipped with a computerized monitoring and control system to ensure repeatability. Single passes were performed to produce spray patterns. The spraying parameters were selected from simulations conducted with a validated numerical model (Ref 27). The stagnation pressure was set to 1.7 MPa for the driving gas. The carrier gas pressure was set to provide a pressure difference of 30 kPa between the powder feeder and the nozzle flow. The powder feeder settings were maintained constant to ensure consistency and repeatability of the powder mass flow rate during different trials. Figure 2 shows the stability of the nozzle inlet static pressure and temperature measurements throughout a cold spray trial. One can see the sudden 30 kPa increase in nozzle inlet static pressure (time 60 s), which corresponds to the activation of the powder feeder and the ensuing pressure increase to ensure the proper feeding of the powder.

### 2.4 Coating and Powder Characterization

The powder composition after cryomilling was evaluated by chemical analysis conducted at a commercial laboratory (Luvak Inc., Boulston, MA). The Al-Mg powder was then examined with a commercially available Coulter LS particle size analyzer (Fullerton, CA). The scanning electron microscopy (SEM) images were obtained using a Philips (Amsterdam, the Netherlands) XL30 FEG microscope, whereas transmission electron microscopy (TEM) inspection was achieved using a Philips CM-12 microscope operated at 120 kV.

The coating quality was evaluated using both quantitative and qualitative analyses. The mass of the powder deposited during the process was determined for each trial. Substrates were weighed before and after the coating procedure using a digital weighting scale (model P-214; Denver Instrument, Denver, CO), and the difference was taken as the deposited mass. Coatings were also examined for defects such as porosity and inter-

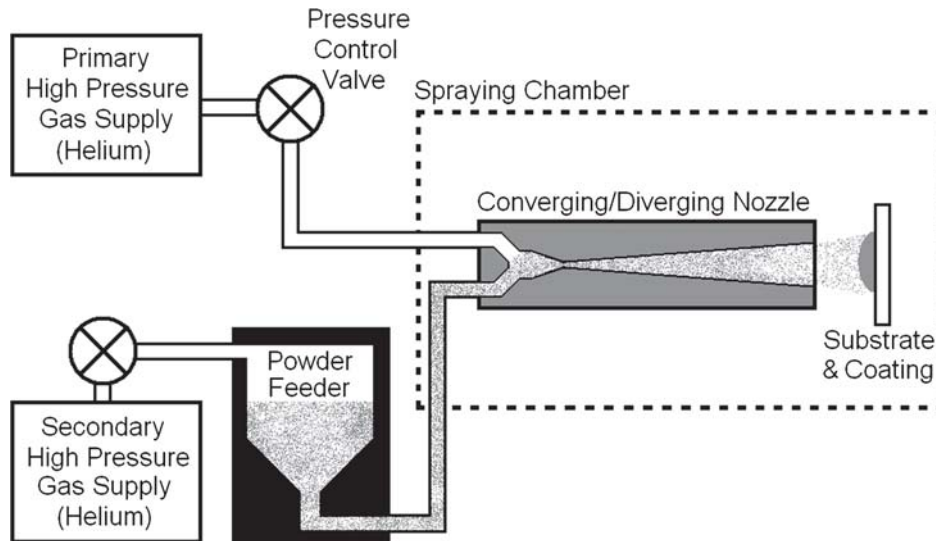


Fig. 1 Schematic of the cold spray facility at the University of Ottawa

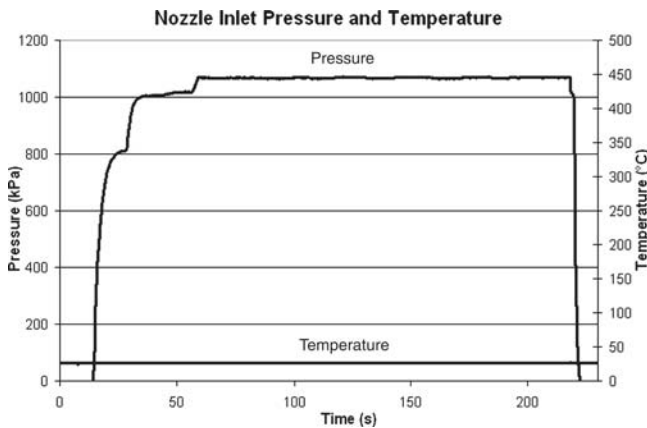


Fig. 2 Pressure and temperature measurements during cold spray trial

lamellar cracks. This was achieved by taking backscattering SEM images of the coating cross sections. Prior to SEM imaging, the test samples were sectioned and polished using standard metallographic techniques. Porosity measurements were performed following ASTM International standard guidelines E 2109-0. Vickers microhardness measurements were performed using a 300 gram-force load. Nanoindentation hardness measurements were performed on the feedstock powder and coatings using an MTS Nanoindenter XP (MTS Nano Instruments, Oak Ridge, TN) with a Berkovich indenter. The reported values are the average of 15 indentations for each sample.

### 3. Results and Discussion

#### 3.1 Powder Characterization

The chemical composition and the particle size distribution of the cryomilled Al-Mg feedstock powder are presented in Table 2 and Table 3, respectively.

Table 2 Composition (wt.%) of the cryomilled Al-Mg alloy

Mg	N	O	C	Fe	Ni	Cr	Mn	Al
6.91	0.38	0.28	0.111	0.12	0.012	0.0041	0.0027	Balance

Table 3 Powder granulometry after cryomilling

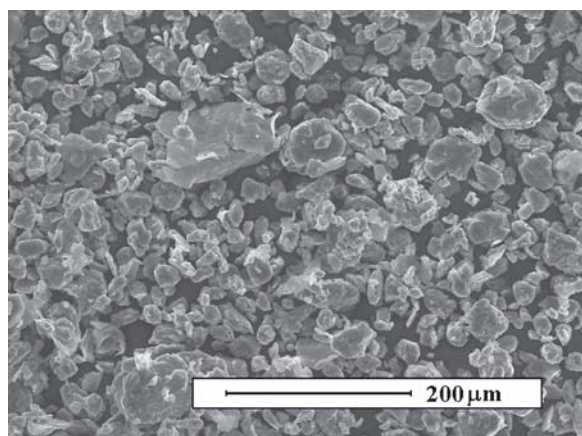
Measurement	Values				
Differential volume, %	10	25	50	75	90
Size, $\mu\text{m}$	<17.1	<24.6	<39.6	<58.0	<80.1

Figure 3 shows an SEM image of the resulting Al-Mg feedstock powder morphology after the cryomilling process. It is observed that the particles are of irregular shape, which is typical of the powder morphology found in cryomilled powders, and that the size distribution is broad. The latter may cause a problem when spraying due to the possible difference in velocity between the larger and smaller particles. Larger particles are expected to be more difficult to accelerate due to their higher inertia, whereas smaller particles may be overly sensitive to disturbances in the flow and may be affected by the shock wave present in front of the substrate (Ref 28). Both of these situations may lead to lower particle velocities on impact with the substrate, and may result in lower deposition efficiency and particle deformation. Finally, the large particle size distribution could lead to spraying complications such as powder-feeding difficulties or nozzle clogging.

The TEM inspection of the cryomilled Al-Mg powder shows that the microstructure is nanocrystalline and that it is composed predominantly of equiaxed grains that are 10 to 30 nm in size, as seen in Fig. 4.

#### 3.2 Effect of Substrate Surface Roughness

The objective of the first series of trials was to identify the effects of the substrate surface preparation, in particular the av-



**Fig. 3** SEM micrograph of cryomilled Al-Mg feedstock powder

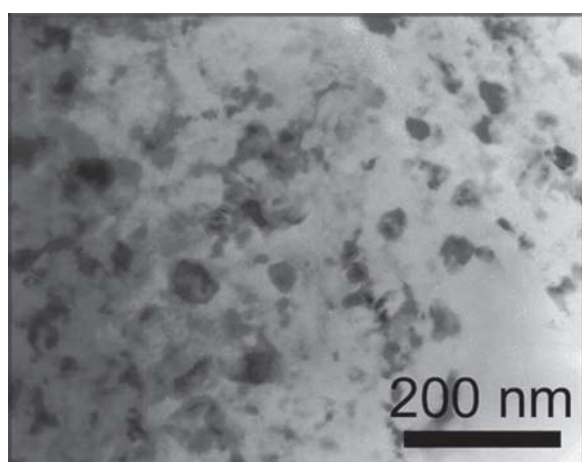
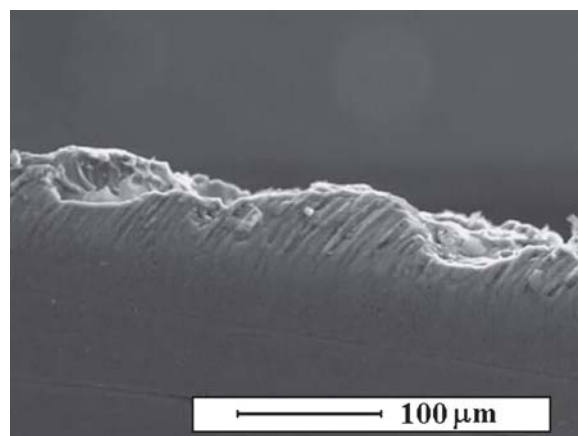


**Fig. 4** TEM micrograph of cryomilled Al-Mg feedstock powder

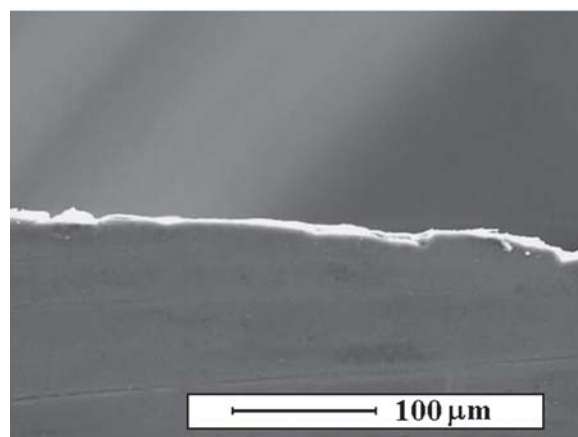
erage surface roughness, using different grit types on the overall quality of the coating.

Measurements showed that the average surface roughness of the substrates prepared with the coarse silica grit was  $316 \pm 57 \mu\text{m}$ , whereas that obtained with the fine glass-bead grit was  $134 \pm 20 \mu\text{m}$  ( $\pm\text{SD}$ ). Coarser grit sizes lead to greater surface roughness during grit-blasting given that each individual impact causes more plastic deformation of the substrate surface. It should also be noted that the silica grit has a higher hardness than the glass bead (hardness 7 and 5.5, respectively, on Mohs abrasive hardness scale). Grits with a greater abrasive hardness can thus convert more energy into plastic deformation of the substrate surface and therefore can further increase its roughness (Ref 29). Figures 5(a) and (b) show the substrate surface profiles obtained on samples prepared with both grits.

The mass deposited during the coating process was examined for the selected trials. The mass deposited on the substrates prepared with the coarse grit was then compared with that of the substrates prepared with the finer grit. The results showed an increase in the mass deposited on the substrates prepared with the coarser grit by approximately 10%. This suggests that greater surface roughness leads to more deposited mass and consequently to better deposition efficiency.



(a)



(b)

**Fig. 5** The SEM micrographs showing the substrate surface roughness resulting from preparation with (a) the coarse silica grit and (b) the fine glass-bead grit

Although the results obtained suggest that surface roughness has an influence on the mass deposited throughout the entire coating process, it is reasonable to assume that it only has an effect on the first few layers of deposited particles. The initial bonding mechanism at the substrate-coating interface, typically defined by adiabatic shear instability and mechanical interlocking of the impinging powder particles with the substrate surface (Ref 2, 30), thus becomes important. It is also necessary to consider that in this study, the nanocrystalline feedstock hardness is significantly higher than that of the aluminum substrate. Vickers microhardness measurements were carried out and showed an average microhardness of  $104 \pm 5$  and  $265.3 \pm 9$  HV, respectively, for the substrates and coatings. Nanoindentation hardness measurements were also performed and showed an average nanohardness of  $3.62 \pm 0.42$  and  $3.58 \pm 0.27$  Gpa, respectively, for the feedstock and coatings. These hardness measurements demonstrate that the feedstock powder and coatings have comparable hardness, and that both are significantly harder than the substrates. As such, when a hard Al-Mg particle collides with the substrate, a large portion of the impact energy is absorbed by the softer substrate material. Both the sprayed particles and substrate deform during the process; however, one can assume that



most of the initial bonding is the result of hard nanocrystalline Al-Mg particles ploughing into the soft substrate. Once the first few layers of sprayed material have been deposited, the substrate properties are altered from those of the soft Al-6061-T651 coating to those of the harder nanocrystalline Al-Mg coating. Plastic deformation of the substrate becomes more difficult due to its higher hardness, and particles can no longer plough into the substrate. The subsequent build up of the coating is then achieved predominantly by plastic deformation of the hard incoming particles, as opposed to the combined plastic deformation of the particles and substrate experienced by the first few layers. Bonding is therefore easier to achieve for a particle striking the soft substrate directly as opposed to particles striking subsequent layers of hard-deposited material. The larger substrate surface roughness obtained with the coarser grit essentially results in a greater substrate surface area, and therefore more particles come into direct contact with the substrate during the spraying of the initial layer. This suggests that a higher deposition efficiency is achieved for the initial layer of sprayed material, which would explain the small increase in mass deposited that was observed in this study. A larger substrate surface roughness thus appears to be beneficial to the initial deposition efficiency of the cold spray process.

Although the substrate surface roughness affects the initial deposition efficiency, it does not influence the coating porosity and interlamellar crack content. Figure 6 shows SEM images of selected coating cross sections that were produced with constant spraying parameters on substrates with different surface roughness. As can be seen, the coating structure is nearly identical in both images. Both coatings exhibit a similar level of porosity (6 and 5%, respectively) and interlamellar crack content. The distribution of defects in both coatings also appears to be homogeneous throughout their thickness. These results suggest that the coating porosity and crack content is independent of the substrate surface roughness, which agrees with the conclusion that once the first few layers of sprayed material have been deposited, the properties of the underlying substrate ultimately become irrelevant to the deposition process. The defects observed in the SEM images result from insufficient compaction of the successive coating layers as well as the lack of plastic deformation of some of the particles. The reason for the relatively high porosity and crack content in these coatings is attributed to the large particle size distribution of the feedstock powder. The modeling results (Ref 28) suggest that the large particles were not accelerated sufficiently due to their higher inertia, and therefore did not reach the desired critical velocity to ensure adequate deformation and bonding. Similarly, the smaller particles were too sensitive to flow disturbances and were likely slowed down significantly by shockwaves, thus leading to insufficient impact velocities. The large particle size range therefore seems to have a detrimental effect on the coating structure given the aerodynamic considerations and constraints. It is, however, possible to mitigate such drawbacks by optimizing the spray parameters.

Figure 7 shows an SEM image of a coating produced with modified spray conditions on a substrate prepared with the glass-bead grit. The modified spraying parameters consisted of a reduced powder feed rate to decrease the particle-loading effects in the jet, which could be considerable in this study given the large particle size distribution. Also, adjustment of the nozzle inlet and powder feeder pressures was performed to minimize

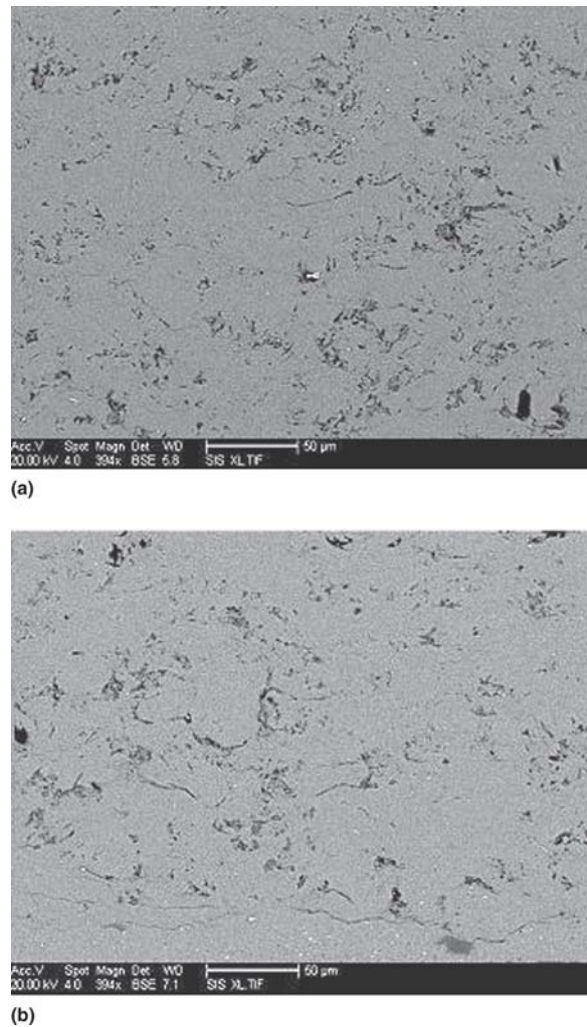


**Fig. 6** The SEM micrographs of cold spray coatings produced on substrates grit blasted with (a) silica (quartz) and (b) glass-bead BT-6

irreversible conditions such as shockwaves in the flow. Compared with the coatings presented in Fig. 6, this coating has a much lower porosity level (1%) and a lower interlamellar crack concentration. The defect distribution in this coating is also homogeneous throughout its thickness. These results indicate that the coating structure is predominantly dependent on spray parameters as opposed to substrate surface preparation. The results also show that the drawbacks associated with the broad particle size distribution of the feedstock can be mitigated by adjusting the spraying parameters.

As discussed previously, the average nanoindentation hardness of the feedstock powder and cold spray Al-Mg coatings were found to be nearly identical. These results demonstrate that the sprayed material has maintained its mechanical properties throughout the cold spray deposition process. The absence of significant heating of the particles has inhibited grain growth throughout the spraying procedure, thus resulting in conservation of the feedstock microstructure, which was revealed by TEM observations of the coating grain size, similar to the initial feedstock powder. It should also be noted that the cold work-

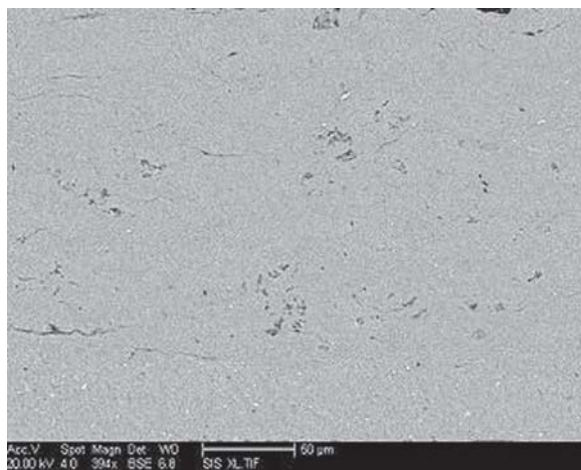
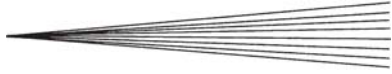


**Fig. 7** SEM micrograph of a cold spray coating produced with modified spraying parameters

hardening effect of the sprayed material as it impacts the substrate is negligible. This is likely attributed to the fact that the nanocrystalline particles have already been extensively cold worked during the cryomilling process, and therefore the introduction of additional dislocations on plastic deformation has a minimal effect on the coating hardness.

### 3.3 Effect of Substrate Thickness

The second set of trials was performed to evaluate the applicability of cold spray coatings on thin substrates. It is believed that the high-velocity gas jet and particle impingement on the substrate may result in critical stresses in unsupported thin substrates. This could cause damage to the substrates such as warping or piercing and could be detrimental to the coating quality. The results obtained for these trials showed that coatings were successfully performed on 1 mm thick aluminum samples without any noticeable damage to the substrate. The substrates did not exhibit any curvature or other visible defects after the surface preparation and the cold spray procedure. Figure 8 shows a comparison of the cross section of four substrates using SEM images to verify whether defects would be introduced within the substrates during the procedures. The four substrates were identical in dimension (10 cm in length, 2 cm in width, and 1 mm in thickness), and each represented a different phase in the coating production process. The first substrate was considered as a reference and consisted of the as-received Al-6061-T651 alloy, the second substrate was manually grit-blasted using the coarse silica grit, the third substrate was also manually grit-blasted and then subjected to the cold spray supersonic jet (no powder particles), and, finally, the fourth substrate was grit-blasted and subjected to the cold spray supersonic jet (with powder particles). It can be seen that all four cross sections are homogeneous, and all appear to be identical to the reference substrate. This suggests that the stresses induced to the substrate by the grit-blasting operation, the supersonic jet, or the impinging particles are not sufficient to cause plastic deformation within the substrate. The force acting on the substrate that resulted from the supersonic gas jet is relatively small. Although the gas velocity is large, the



gas jet cross-sectional area and density remain small. According to calculations and given substrate dimensions, the thrust ( $T = \rho_e V_e^2 A_e$ , where the subscript  $e$  refers to the exit plane of the nozzle) generated by the nozzle jet that impinges on the substrate induces a maximal bending stress of 40.9 MPa. When compared with the tensile yield strength of the substrate material, it can be seen that such applied stresses would only generate elastic deformation, and therefore no permanent curvature of the substrate is expected. Alternatively, the evaluation of the stresses caused by the impingement of particles on the substrates cannot be achieved so easily. Evaluating the stresses resulting from the deformation and bonding that occurs on impact is quite complex and is not addressed in this article. However, given that the size of a single powder particle and its corresponding mass are very small, the momentum of the particle on impact is only large enough to create local plastic deformation at the surface of the substrate, and is therefore insufficient to cause damage throughout the substrate thickness. Figure 9 is an SEM image of the surface of a coating showing a deformed particle and a crater formed in the substrate as a result of particle impact. It shows that the size of the region affected by the impingement of particles is typically of the same order of magnitude as the size of the impinging particles, which agrees with other modeling and experimental work (Ref 9). Plastic deformation of the substrate resulting from the impact of impinging particles is thus confined to the substrate surface. It seems that the predominant concern when considering thin substrates would thus be the bending stresses resulting from the thrust of the supersonic jet, and therefore the limiting criteria would be the moment of inertia of the substrate cross section. Assuming that this is true, the minimal substrate thickness can be approximated for a substrate with fixed dimensions. Plastic deformation and the failure of the substrate could be predicted based on the yield strength and ultimate tensile strength of the substrate material, respectively. For the aluminum substrates considered in this study, the minimal allowable thickness at which plastic deformation and therefore damage would occur is 0.39 mm. At this thickness, the impingement of particles would not likely cause damage throughout the substrate thickness given that the particles are typically much smaller.

The quality of the thin substrate coatings was evaluated. Figure 10 shows the backscattered SEM images for two coatings produced with identical spraying conditions on substrates of different thickness. It should be noted that these coatings were produced prior to determining the modified spray parameters. This explains the relatively large porosity content and crack density. It is apparent from these images that there is no significant change in structure between the two coatings because they exhibit similar porosities (9%) and interlamellar crack densities. It should be noted that the small increase in porosity when compared with the trials performed on thicker substrates (as shown in Fig. 6) is the direct result of different spraying parameters as opposed to substrate thickness.

## 4. Conclusions

Nanocrystalline Al-Mg coatings were produced using the cold spray process. The feedstock powder was characterized by a broad particle size distribution and was sprayed as-received.



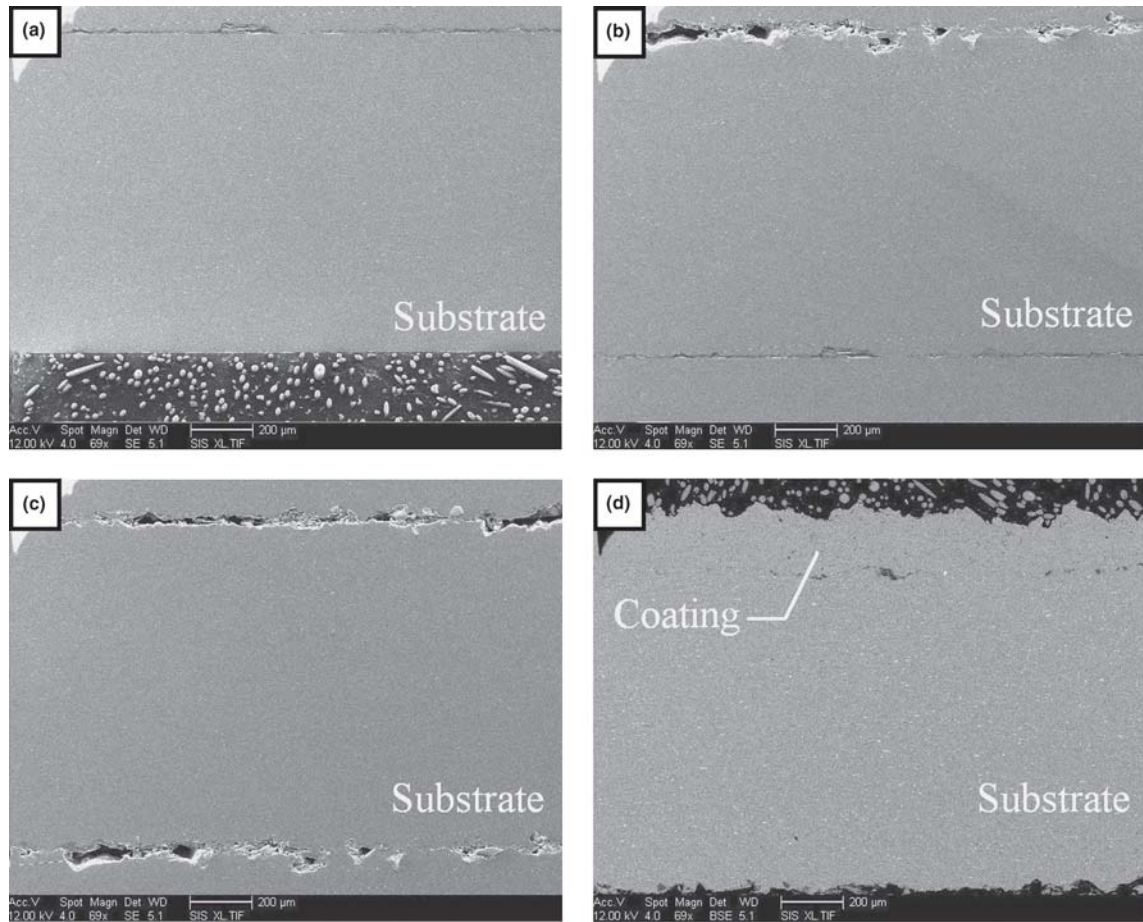


**Fig. 8** The SEM micrographs of substrate cross sections (a) as-received, (b) grit-blasted, (c) grit-blasted and subjected to spray jet (without particles), and (d) grit-blasted and subjected to spray jet (with particles)

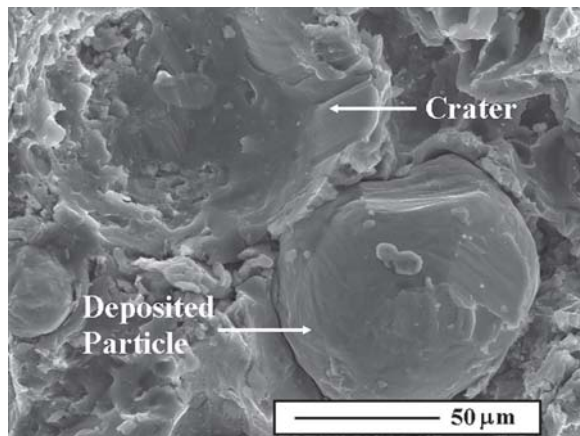


**Fig. 9** An SEM micrograph of a coating surface showing a deformed particle and a crater formed in the substrate from a particle impact

Experimental results showed that the cold spray process was successful in producing high-quality coatings with unsieved feedstock powder and that the undesirable aerodynamic implications of the large particle size distribution could be overcome by the optimization of the spray parameters. Nanoindentation

hardness measurements and TEM inspection demonstrated that the microstructure of the original feedstock powder was conserved throughout the cold spray process, and that no increase in hardness due to cold working of the particles was observed.

Trials were performed to evaluate the effect of substrate average roughness on the overall coatings quality. Substrates were prepared by grit blasting using two different types of grit material. Measurements of the deposited mass were performed, and the microstructure of the coatings was evaluated by SEM. The results indicated that the use of coarser grit sizes led initially to the slightly higher mass deposited as a result of increased substrate roughness. The substrate surface roughness was shown to have an effect on the mass deposited and the deposition efficiency of only the first few layers of deposited material, but not on subsequent layers resulting from coating build up. A high surface roughness provides a larger substrate surface area onto which hard particles can impact and adhere. Ploughing of the hard particles into the soft substrate seems to be favorable for the initial deposition process. These factors all contribute to the small increase in mass deposited and the deposition efficiency observed on the high-roughness substrates. The different grit types did not have any noticeable effect on the coating structure.

Trials were also performed to determine whether cold spray could be used to produce high-quality coatings on thin sub-

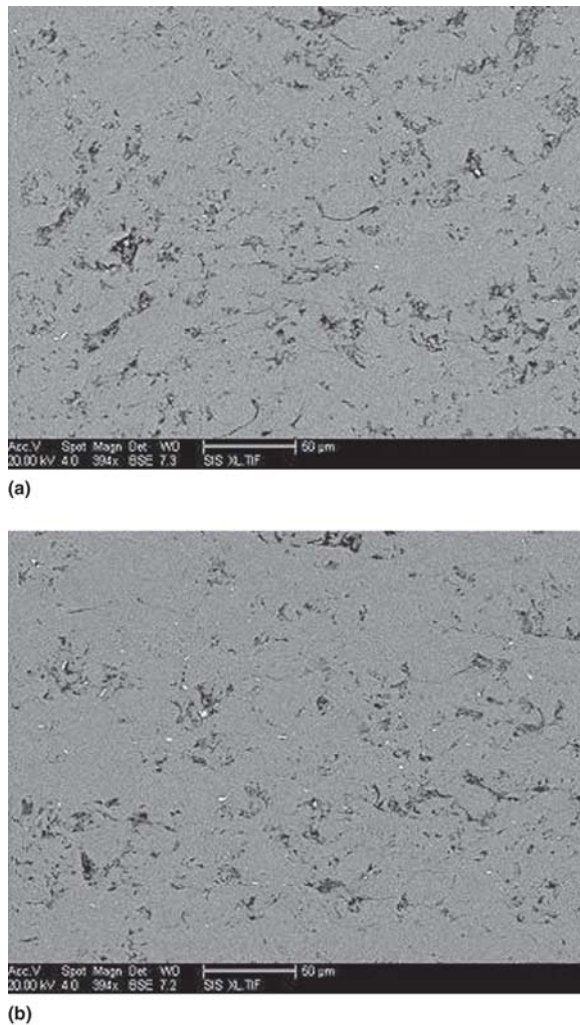


**Fig. 10** The SEM micrographs of cold spray coatings produced on substrates with different thickness: (a) 1 mm; (b) 6.35 mm

strates. Two different substrate thicknesses were considered. The results showed that cold spray can be successfully used to produce coatings on thin parts without causing significant and apparent damage to the substrate. It was shown, however, that the thrust of the supersonic jet is mostly susceptible to causing damage to the substrate as opposed to particle impingement, and therefore substrate thickness limitations should be considered. The substrate thickness was shown to have no noticeable effect on the deposition efficiency or the resulting coating structure.

### Acknowledgments

The authors wish to acknowledge Natural Sciences and Engineering Research Council of Canada (NSERC) for their financial support as well as the participation of Dr. C. Bampton from Rocketdyne Propulsion & Power-Boeing for providing the nanocrystalline Al-Mg powder. The authors would also like to thank Brent Cotter, Leo Denner, and James MacDermid from the University of Ottawa for their assistance with the cold spray experimental equipment. The authors would like to acknowledge Eric Sansoucy and Karen Taylor from the University of Ottawa for their help in the Cold Spray Laboratory.

### References

1. A.P. Alkhimov, A.N. Papyrin, V.F. Kosarev, N.I. Nesterovich, and M.M. Shushpanov, Gas-Dynamic Spraying Method for Applying a Coating, U.S. Patent 5,302,414, April 12, 1994
2. T.H. Van Steenkiste, J.R. Smith, and R.E. Teets, Aluminum Coatings via Kinetic Spray with Relatively Large Powder Particles, *Surf. Coat. Technol.*, 2002, **154**, p 237-252
3. C.-J. Li, W.-Y. Li, and H. Fukanuma, Impact Fusion Phenomenon During Cold Spraying of Zinc, *Thermal Spray 2004: Advances in Technology and Application*, ASM International, May 10-12, 2004 (Osaka, Japan), ASM International, 2004, p 1129 p
4. C. Borchers, F. Gärtner, T. Stoltenhoff, and H. Kreye, Microstructural and Macroscopic Properties of Cold Sprayed Copper Coatings, *J. Appl. Phys.*, 2003, **93**, p 10064-10070
5. R. Morgan, P. Fox, J. Pattison, C. Sutcliffe, and W. O'Neill, Analysis of Cold Gas Dynamically Sprayed Aluminum Deposits, *Mater. Lett.*, 2004, **58**, p 1317-1320
6. C.-J. Li and W.-Y. Li, Deposition Characteristics of Titanium Coating in Cold Spraying, *Surf. Coat. Technol.*, 2003, **167**, p 278-283
7. R.S. Lima, J. Karthikeyan, C.M. Kay, J. Lindemann, and C.C. Berndt, Microstructural Characteristics of Cold-Sprayed Nanostructured WC-Co Coatings, *Thin Solid Films*, 2002, **416**, p 129-135
8. L. Ajdelsztajn, B. Jodoin, G.E. Kim, J.M. Schoenung, and J. Mondoux, Cold Spray Deposition of Nanocrystalline Aluminum Alloys, *Metall. Mater. Trans. A*, 2005, **36**, p 657-666
9. R.C. Dykhuizen, M.F. Smith, D.L. Gilmore, R.A. Neiser, X. Jiang, and S. Sampath, Impact of High Velocity Cold Spray Particles, *J. Thermal Spray Technol.*, 1999, **8**(4), p 559-564
10. H. Assadi, F. Gärtner, T. Stoltenhoff, and H. Kreye, Bonding Mechanism in Cold Gas Spraying, *Acta Mater.*, 2003, **51**, p 4379-4394
11. A.P. Alkhimov, A.I. Gudilov, V.F. Kosarev, and N.I. Nesterovich, Specific Features of Microparticle Deformation Upon Impact on a Rigid Barrier, *J. Appl. Mech. Tech. Phys.*, 2000, **41**(1), p 188-192
12. M. Grujicic, J.R. Saylor, D.E. Beasley, W.S. DeRosset, and D. Helfritsch, Computational Analysis of the Interfacial Bonding Between Feed-Powder Particles and the Substrate in the Cold-Gas Dynamic-Spray Process, *Appl. Surf. Sci.*, 2003, **219**, p 211-227
13. T. Schmidt, F. Gärtner, H. Assadi, and H. Kreye, Development of a Generalized Parameter Window for Cold Spray Deposition, *Acta Mater.*, 2006, **54**, p 729-742
14. P. Richer, B. Jodoin, and L. Ajdelsztajn, 'Characteristics of Cold Sprayed Coatings Using Nano-Aluminum and Nano-Nickel Powders,' *16th Canadian Materials Science Conference*, Ottawa, ON, Canada, June 2004
15. E. Sansoucy, B. Jodoin, and L. Ajdelsztajn, Conventional and Nano-Structured Nickel Coatings Produced by Cold Spray Processing, *16th Canadian Materials Science Conference*, Ottawa, ON, Canada, June 2004
16. L. Ajdelsztajn, B. Jodoin, and J.M. Schoenung, Synthesis and Mechanical Properties of Nanocrystalline Ni Coatings Produced by Cold Gas Dynamic Spraying, *Surf. Coat. Technol.*, in press (corrected proof available online February 28, 2006)
17. L. Ajdelsztajn, A. Zuniga, B. Jodoin, and E. Lavernia, Cold Gas Dynamic Spraying of a High Temperature Al Alloy, *Surf. Coat. Technol.*, in press (corrected proof available online July 19, 2005)
18. E. Gaffet, N. Malhouroux, and M. Abdellaoui, Far from Equilibrium Phase Transition Induced by Solid State Reaction in the Fe-Si System, *J. Alloys Compd.*, 1993, **194**, p 339-360
19. L. Ajdelsztajn, F. Tang, G.E. Kim, V. Provenzano, and J.M. Schoenung, Synthesis and Oxidation Behavior of Nanocrystalline MCrAlY Bond Coatings, *J. Thermal Spray Technol.*, 2005, **14**(1), p 23-30
20. L. Ajdelsztajn, J. Lee, K. Chung, F.L. Bastian, and E.J. Lavernia, Synthesis and Nanoindentation Study of High-Velocity Oxygen Fuel Thermal-Sprayed Nanocrystalline and Near-Nanocrystalline Ni Coatings, *Metall. Mater. Trans. A*, 2002, **33**, p 647-655
21. T. Stoltenhoff, H. Kreye, H.R. Richter, and H. Assadi, Optimization of the Cold Spray Process, *Thermal Spray 2001: New Surfaces for a New Millennium*, C.C. Berndt, K.A. Khor, and E.F. Lugscheider, Ed., May 28-30, 2001 (Singapore), ASM International, 2001, 1381 p
22. T. Stoltenhoff, H. Kreye, and H.J. Richter, An Analysis of the Cold Spray Process and Its Coatings, *J. Thermal Spray Technol.*, 2002, **11**(4), p 542-550
23. J. Vlcek, L. Gimeno, H. Huber, and E. Lugscheider, A Systematic Ap-



- proach to Material Eligibility for the Cold Spray Process, *J. Thermal Spray Technol.*, 2005, **14**(1), p 125-133
24. J. Vlcek, H. Huber, H. Voggenreiter, A. Fischer, E. Lugscheider, H. Hallen, and G. Pache, Kinetic Powder Compaction Applying the Cold Spray Process: A Study on Parameters, *Thermal Spray 2001: New Surfaces for a New Millennium*, C.C. Berndt, K.A. Khor, and E.F. Lugscheider, Ed., May 28-30, 2001 (Singapore), ASM International, 2001, 1381 p
  25. F. Zhou, X.Z. Liao, Y.T. Zhu, S. Dallek, and E.J. Lavernia, Microstructural Evolution During Recovery and Recrystallization of a Nanocrystalline Al-Mg Alloy Prepared by Cryogenic Ball Milling, *Acta Mater.*, 2003, **51**, p 2777-2791
  26. C. Suryanarayana, Nanocrystalline Materials, *Int. Mat. Rev.*, 1995, **40**, p 41-64
  27. B. Jodoin, F. Raletz, and M. Vardelle, Cold Spray Modelling and Validation Using an Optical Diagnostic Method, *Surf. Coat. Technol.*, 2006, **200**, p 4424-4432
  28. B. Jodoin, Cold Spray Nozzle Mach Number Limitation, *J. Thermal Spray Technol.*, 2002, **11**(4), p 496-507
  29. E. Rabinowicz, An Adhesive Wear Model Based on Variations in Strength Values, *Wear*, 1980, **63**, p 175-181
  30. T.H. Van Steenkiste, Kinetic Spray: A New Coating Process, *Key Eng. Mater.*, 2001, **197**, p 59-86